Integrating Simulations and Experiments To Predict Sheet Resistance and Optical Transmittance in Nanowire Films for Transparent Conductors

Rose M. Mutiso,[†] Michelle C. Sherrott,[†] Aaron R. Rathmell,[‡] Benjamin J. Wiley,[‡] and Karen I. Winey[†,*]

[†]Department of Materials Science and Engineering, University of Pennsylvania, Philadelphia, Pennsylvania 19104, United States, and [‡] Department of Chemistry, Duke University, Durham, North Carolina 27708, United States

ABSTRACT Metal nanowire films are among the most promising alternatives for next-generation flexible, solution-processed transparent conductors. Breakthroughs in nanowire synthesis and processing have reported low sheet resistance ($R_s \leq 100$ Ω/sq) and high optical transparency (%$T > 90$%). Comparing the merits of the various nanowires and fabrication methods is inexact, because R_s and %T depend on a variety of independent parameters including nanowire length, nanowire diameter, areal density of the nanowires and contact resistance between nanowires. In an effort to account for these fundamental parameters of nanowire thin films, this paper integrates simulations and experimental results to build a quantitatively predictive model. First, by fitting the results from simulations of quasi-2D rod networks to experimental data from well-defined nanowire films, we obtain an effective average contact resistance, which is indicative of the nanowire chemistry and processing methods. Second, this effective contact resistance is used to simulate how the sheet resistance depends on the aspect ratio (L/D) and areal density of monodisperse rods, as well as the effect of mixtures of short and long nanowires on the sheet resistance. Third, by combining our simulations of sheet resistance and an empirical diameter-dependent expression for the optical transmittance, we produced a fully calculated plot of optical transmittance *versus* sheet resistance. Our predictions for silver nanowires are validated by experimental results for silver nanowire films, where nanowires of $L/D > 400$ are required for high performance transparent conductors. In contrast to a widely used approach that employs a single percolative figure of merit, our method integrates simulation and experimental results to enable researchers to independently explore the importance of contact resistance between nanowires, as well as nanowire area fraction and arbitrary distributions in nanowire sizes. To become competitive, metal nanowire systems require a predictive tool to accelerate their design and adoption for specific applications.

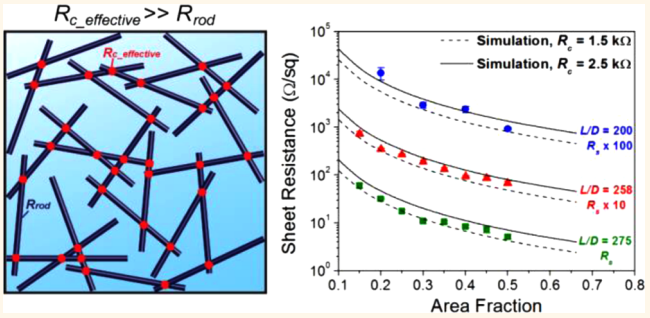

KEYWORDS: simulations · transparent conductor · nanowires · silver · sheet resistance · contact resistance

Transparent conductors (TCs) enable today's ubiquitous flat panel displays and touch screen technologies, as well as numerous emerging applications such as electrodes in thin-film solar cells, organic light emitting diodes (OLEDs), e-paper, sensors, electrostatic shielding and antistatic coatings.[1] Across all application areas, two critical performance criteria for TCs are the optical transmittance (%T) and sheet resistance (R_s). Very high optical transmittance in the visible region (≥90%) is a typical requirement for most applications, whereas R_s can vary across a broad range depending on the specific application. For example, TCs for electrodes in solar cells and OLEDs require very low R_s (<10 Ω/sq), whereas R_s values of ~100 Ω/sq are acceptable for many touch screen applications, and static dissipation and electromagnetic shielding requirements are typically >10^3 Ω/sq.[1−3] Indium tin oxide (ITO) has dominated the field of transparent conductors due to its high performance,[2,4] although the brittleness of ITO renders it unsuitable for next generation flexible display applications. The search is underway for

* Address correspondence to winey@seas.upenn.edu.

Received for review April 29, 2013 and accepted August 9, 2013.

Published online 10.1021/nn403324t

new material alternatives for high performance TC applications that exhibit very high optoelectronic performance (%T > 90% and $R_s \leq 100$ Ω/sq), as well as meet important criteria such as affordability, flexibility and compatibility with low-temperature and large area solution processing.[3]

Currently, the most important material systems being explored as new TCs are conducting polymers[5,6] and networks of highly conductive nanoscale materials such as carbon nanotubes,[7−11] graphene flakes,[12,13] and metal nanowires.[14−24] Conducting polymers such as poly(3,4-ethylenedioxythiophene) poly(styrenesulfonate) underperform relative to ITO for applications requiring low sheet resistances and also suffer from stability issues.[1,6] Random networks of carbon nanotubes are widely studied but typically exhibit lower performance than ITO due to large contact resistances between nanotubes, as well as high levels of impurities and dispersity.[1] Graphene-based TCs are evolving quickly, but have yet to meet the necessary performance criteria when processed from solution due to numerous grain boundaries and defects.[1,12] Random networks of metal nanowires are widely considered to be the most promising candidates with performances on par with ITO and competing amorphous oxides.[3,25] Metal nanowire films are compatible with low-temperature solution processing and large-area deposition, which can reduce cost and make them ideal for emerging flexible TC applications. Silver nanowire thin-films have displayed the best performance[14−18,24] and have entered the market as the first commercially available wet-processed TCs for touch screen applications.[26,27]

To date, very few studies in the literature attempt to systematically correlate the nanowire properties and the structure of nanowire films to their final properties. The most systematic experimental study so far was conducted by Bergin *et al.*,[15] who combined experiments and optical simulations to study the properties of silver nanowire films as a function of the nanowire length, diameter and area coverage. Experimentally, they observed a strong dependence on R_s on both the length and areal density of nanowires, results that are consistent with theoretical predictions for 2D widthless-sticks systems.[28−30] In addition, the %T of the networks was inversely proportional to the area coverage of the nanowires. Sorel *et al.*[31] studied the effect of silver nanowire length and diameter on the optoelectronic properties, observing a strong effect of nanowire length on network conductivity but not on transmittance. Coleman and co-workers[3,32] related %T and R_s nanowire films to the approximate film thickness by extrapolating from bulk to percolative behavior, but this semiempirical approach fails to explicitly account for nanowire dimensions and network structure which strongly govern the performance, particularly in sparse networks. A detailed analysis of their model will be provided later in this paper.

While there is broad consensus in the field that metal nanowires are among the most promising nanoscale material for transparent conductors,[1,3,25] exploiting their full potential and enabling their rapid adoption requires robust predictive models. The optoelectronic properties of metal nanowire mats depend on a myriad of characteristics including nanowire structure (length, diameter, size dispersity, composition, *etc.*) and the overall network morphology (areal density, dispersion, orientation, *etc.*). Predictive and quantitative models of the optoelectronic properties of metal nanowire promise to provide guidance for nanowire synthesis and network fabrication and thereby facilitate reliable and rapid design of engineered networks with optimized properties for specific applications. To date, several simulations studies have modeled the electrical properties of 2D networks of rodlike nanoscale fillers.[28,33−37] These studies are mainly targeted at carbon nanotube films and their primary focus is the critical percolation phenomena, although Behnam and Ural[33] and Kocabas *et al.*[34] related their simulations to experiments to elucidate geometry scaling behavior in CNT-based thin-film transistors. The only attempt to explicitly simulate the network sheet resistance to date was conducted by Lee *et al.*,[14] who used a highly idealized periodic network structure that is inconsistent with the morphology of random nanowire networks.

In this paper, we present the first simulations of the sheet resistance of thin-film metal nanowire networks as a function of the nanowire size (length and diameter), size dispersity and areal density. We tune a single parameter in the simulations, the effective average contact resistance between two nanowires ($R_{c\_effective}$), to fit experimental values of the sheet resistance of nanowire films as a function of areal density. With the use of this fitting parameter, our simulations then quantitatively predict sheet resistance as a function of nanowire size, size dispersity and areal density. Further, by combining our simulations of sheet resistance and a recently published empirical expression for optical transmittance, we report the first fully calculated plot of optical transmittance *versus* sheet resistance, the two parameters that define performance in the field of transparent conductors. For the silver nanowires investigated here, we find $R_{c\_effective} = 2$ kΩ and $L/D > 100$ is required for low sheet resistances ($R_s \leq 100$ Ω/sq) at modest nanowire densities. Moreover, we observe that higher-L/D rods ($L/D > 400$) and intermediate areal densities are required to simultaneously optimize the optical transmittance and the sheet resistance to $R_s \leq 100$ Ω/sq at %T > 90%. These predictions are consistent with reported experimental results for high-performance silver nanowire films, demonstrating the ability of our simulations to capture important experimental trends. Our integrated simulation and experimental

methodology extracts $R_{c\_effective}$, thereby enabling comparisons between nanowires of different compositions or networks fabricated by distinct means in a manner that is deconvoluted from the dimensions of the nanowires and the areal densities of the networks. This direction-setting contribution creates a comprehensive framework for understanding structure–property relationships in metal nanowire networks, thereby guiding future experimental work and accelerating the development of these promising systems.

RESULTS AND DISCUSSION

Extracting $R_{c\_effective}$ from Experimental Data. To simulate the sheet resistance of quasi-2D nanowire networks, we employ a two-step approach. First, random assemblies of rods are generated using a Monte Carlo process and a clustering analysis performed to identify percolated or spanning rod clusters. Second, the current across the sample is calculated using a random resistor network approach[38] to discretize the rod network and Kirchoff's current law equations are solved at each node. We have previously used this simulation approach in three-dimensional networks to explore the effects of rod orientation, aspect ratio, and size-dispersity on the electrical conductivity of polymer nanocomposites containing cylindrical nanofillers such as carbon nanotubes and metal nanowires.[39−41] In those studies, only the critical concentrations at the electrical percolation threshold were compared quantitatively to experimental results. In the current work, we adapt our 3D simulation approach to model the sheet resistance of quasi-2D nanowire films by confining the rods to a thin film. The quasi-2D rod networks are quite appropriate for nanowire films when the networks are sparse and L/D is larger than ~20, as typical for transparent conductors. Representative renderings from the quasi-2D simulations are provided in Supporting Information (Figure SI-1) and illustrate the large systems sizes used in the simulations.

Figure 1 shows the sheet resistances as a function of the area fraction from three sets of experimental data from model silver nanowire (Ag NW) films composed of nanowires having diameters of 50, 84, and 75 nm, corresponding to nanowires with L/D = 200, 258, and 275, respectively. The area fraction (AF) is defined as the number density of the nanowires in a film multiplied by the projected area of a nanowire. We simulate networks with rods of the same dimensions and compute the sheet resistance. To fit the simulations to the experimental results, we adjust the one free variable in the simulation, namely, the effective average contact resistance between two nanowires, $R_{c\_effective}$. The agreement between the experiments and simulation is quite good indicating that our simulations quantitatively capture the influence of nanowire dimensions and area fraction on sheet resistance.

Before proceeding, we enumerate several attributes of our simulations. The rods interpenetrate; this

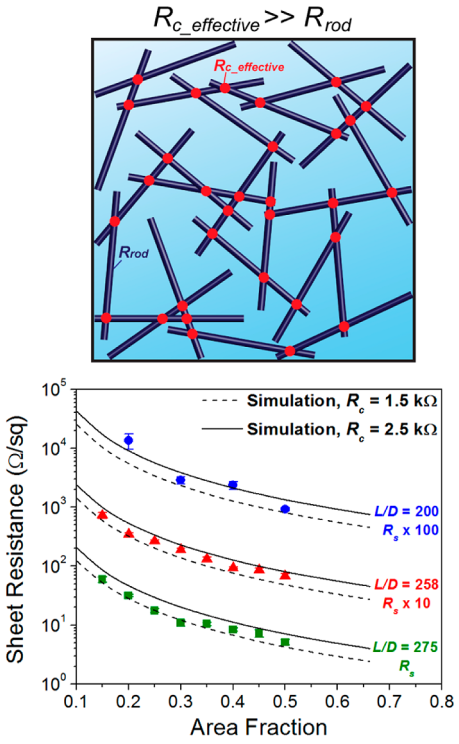

Figure 1. Schematic illustrates a percolated network of monodisperse rods in which the resistance at nanowire–nanowire junctions (red dots) dominates ($R_c \gg R_{rod}$). Experimental sheet resistance (R_s) for silver nanowire thin films (points) as a function of the area fraction (AF) for three L/D values as indicated. Sheet resistance from quasi-2D simulations of rods with specified L and D use an effective contact resistance ($R_{c\_effective}$) to fit the simulations to the experimental data and best fits correspond to $R_{c\_effective}$ = 1.5 kΩ (dashed lines) and 2.5 kΩ (solid lines).

is a widely accepted approximation[41−46] that we have previously shown has little impact on the percolation threshold when compared to experiment.[40] The rods are rigid, straight cylinders, which is an appropriate representation for experimentally typical nanowires with diameters of 40–100 nm and lengths <20 μm. One contact resistance, R_c, is assigned to all rod–rod junctions in the system irrespective of the contact area. This assumption has previously been applied to nanotube systems even though the junction resistances are expected to vary widely due to the presence of both metallic and semiconducting CNTs,[28,33,35,36,47] and is certainly more appropriate between metal nanowires. Finally, all the resistance in our networks arises from the contacts and the rods themselves have no internal resistance ($R_{rod} = 0$). This assumption is credible for our Ag NW films, because the quality of the fit is good, Figure 1. Moreover, the percolation conductivity exponent is 1.75 (Figure SI-2) and this exponent is consistent with transport dominated by contact resistance ($R_c \gg R_{rod}$).[36,37] In a complementary study of critical behavior in these quasi-2D systems, a percolation conductivity exponent of two is observed at higher rod densities.[48] Naturally, the specifics of nanowire synthesis and nanowire film fabrication and processing

can alter the extent to which the $R_c \gg R_{nw}$ assumption is legitimate, but the quality of the fits in Figure 1 and conductivity exponent in Figure SI-2 indicate that the contact resistance dominates here.

We obtain the best fit to experimental results when $R_{c\_effective}$ is between 1.5 and 2.5 kΩ (Figure 1). Importantly, the same $R_{c\_effective}$ range fits all three experimental data sets for Ag NWs with D_{nw} = 50−84 nm, which is consistent with the expectation that $R_{c\_effective}$ has only minimal sensitivity to diameter across a narrow range. For comparison, contact resistance values reported in the literature from electrical measurements of crossed Ag NW junctions with average diameter $D_{nw} \approx 40-80$ nm are ~8 kΩ for plasmonically welded silver junctions[49] and ~0.5 kΩ for Ag NWs coated with gold *via* electrochemical annealing.[18] These experimental values correspond to isolated junctions. In contrast, the $R_{c\_effective}$ is extracted from our simulations comprising 10^3 to 10^6 rods *via* fits to experimental nanowire films containing a diverse collection of nanowire junctions. The extracted value of $R_{c\_effective}$, as the only adjustable parameter in our simulations, encompasses both the various simplifying assumptions in the simulation and the nonidealities in the experimental system (size dispersity, *etc.*) in addition to approximating R_c.

The $R_{c\_effective}$ is a valuable and previously inaccessible parameter. First, using $R_{c\_effective}$, we can reliably obtain quantitative predictions of Ag NW films prepared by comparable methods as a function of areal density, nanowire size (length and diameter), size dispersity, and nanowire orientation; this is demonstrated in part below. Second, by finding $R_{c\_effective}$ for distinct nanowires and fabrication methods, one could reliably assess new metal nanowire materials and processing methods independent of *L*/*D* and area fraction variations. This integrated simulation and experimental approach could profoundly increase the speed at which new transparent conductors are developed for specific applications.

Quantitative Predictions of R_s. Now we apply $R_{c\_effective}$ = 2 kΩ in our simulations to predict the dependence of the sheet resistance (R_s) on the nanowire aspect ratio (*L*/*D*) and area fraction (AF) in silver nanowire films (Figure 2). We simulate nanowire networks over a broad aspect ratio range *L*/*D* = 25−800, where all the rods have D_{rod} = 50 nm and the lengths vary (L_{rod} = 1.25−40 μm). For each *L*/*D*, the R_s follows 3 stages that are typical of percolative behavior: (1) high resistance network at low nanowire densities (AF = 0.01 when *L*/*D* = 800), (2) rapid decrease in R_s in the critical region in the vicinity of the percolation threshold (AF_c), and (3) weakening AF dependence at high nanowire densities when the network is well established.

The results presented in Figure 2 are the first theoretical predictions of the R_s-dependence on nanowire *L*/*D* and areal density. We observe a very strong

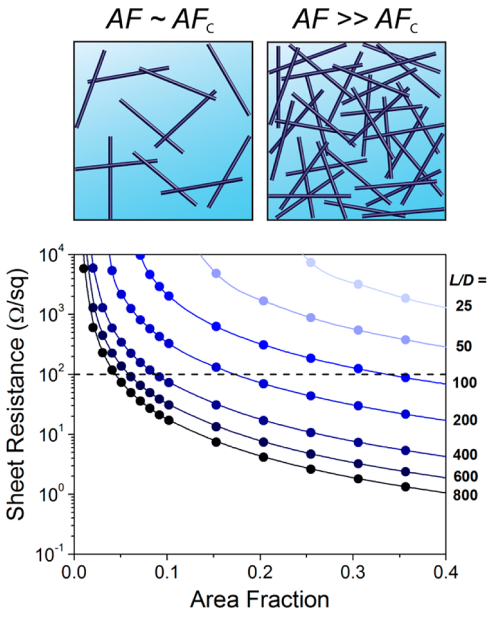

Figure 2. Schematics illustrate two percolated networks of monodisperse rods with nanowire area fractions near or far above the critical area fraction for percolation (AF_c). Sheet resistance from simulations as a function of *L*/*D* and area fraction of the rods in nanowire films using an effective average contact resistance $R_{c\_effective}$ = 2 kΩ and constant D_{rod} = 50 nm. The dashed line indicates the desired performance criterion $R_s \leq 100$ Ω/sq for high performance applications.

aspect-ratio dependence of the sheet resistance. For dense networks, R_s at a given area fraction drops by a factor of ~ 4 when the aspect ratio doubles. Moreover, increasing *L*/*D* continues to be valuable even to very high *L*/*D* = 800. For many applications, the maximum allowed sheet resistance is 100 Ω/sq, and these results find that *L*/*D* > 100 is required to meet this criterion at moderate area fractions (AF < 0.4, D_{rod} = 50 nm). These predictions are most reliable, of course, for silver nanowire films prepared using comparable methods and comprising Ag NWs with $D_{nw} \approx 40-100$ nm and lengths <20 μm, because these are consistent with our determination of $R_{c\_effective}$ (Figure 1). Nevertheless, the findings in Figure 2 provide valuable insights. Specifically, our findings motivate the aggressive pursuit of improved synthetic methods to produce ultra-high-aspect-ratio nanowires to optimize the sheet resistance of nanowire-based TCs.

The strong aspect-ratio dependence of R_s in Figure 2 is qualitatively consistent with percolation studies of high aspect ratio rods and quantitatively consistent with experiments of metal nanowires. In theories of widthless 2D sticks, the critical number density of sticks (N_c) required to form percolated network is inversely proportional to L_{stick}^2 ($N_c \propto 1/L_{stick}^2$).[50] Thus, longer sticks yield better-connected networks, resulting in higher conductivities at lower number density of sticks, which is consistent with our findings in Figure 2.

The finding that $L/D > 100$ is required for $R_s \leq 100\ \Omega$/sq at modest nanowire densities is consistent with recent experimental results from Bergin *et al.*,[15] who observe unacceptable performance for silver nanowire films with $L/D = 37$ and 73, and good performance for silver nanowire films with $L/D = 182$ and 375. In contrast, other researchers[14,16] have reported similarly low R_s values for silver nanowires with surprisingly modest $L/D \approx 80$, but here the distributions in L are asymmetrical and heavily skewed toward longer lengths. A few higher-L/D nanowires can appreciably increase the network conductivity relative to monodisperse or symmetric size distributions with the same number-averaged mean length. The effect of skewing the size distribution of nanowires toward longer lengths will be discussed later in this manuscript.

Another interesting observation from Figure 2 is that the strong effect of L/D in determining the R_s persists even for very dense networks (See Figure SI-3 for simulated R_s up to 70% area coverage), indicating that nanowire dimensions and the resulting network structure are important even for dense networks. Similarly, De *et al.*[16] observed that conductivity of dense silver nanowire networks transitions from percolative to bulk-like behavior with increasing thickness, saturating at a constant conductivity value ~8% of the bulk conductivity of silver for very thick films. However, as their study was limited to nanowires with $L/D \approx 80$, they do not report on the effect of the nanowire dimensions on this saturation conductivity value. Our results show that the minimum sheet resistance achievable for a dense nanowire network is strongly dependent on L/D. For example, a network comprising the lowest-L/D rods ($L/D = 25$) at high area fraction (AF > 0.4) has an R_s value that is 3 orders of magnitude higher than that of a network comprising the highest-L/D rods ($L/D = 800$). This behavior is expected in our contact-resistance dominated system ($R_c \gg R_{nw}$) as there is a very high penalty for additional contacts[28] and the number of contacts per rod is proportional to the number of rods.[36,37] Thus, at a fixed area fraction networks of high-L/D rods outperform those of low-L/D rods as the former can form networks more efficiently with fewer rods and hence fewer rod−rod contacts.

Effect of Nanowire Size Dispersity on R_s. Figure 2 demonstrates that very high-L/D nanowires are the most promising candidates for high-performance applications when nanowires are identical in size. A significant advantage of having a verified simulation method that predicts R_s as a function of nanowire size and network structure is the ability to explore nanowire systems with arbitrary size variations in L_{rod} and D_{rod}. In our recent simulations of 3D rod networks, we explored Gaussian distributions in nanowire size (L, D, or both) and bi-disperse mixtures of rods (fixed D and two lengths).[41] To demonstrate this capability in our quasi-2D model, we simulate a rod network using a bi-disperse distribution of rod lengths. We define reference rods with $L/D = 50$ ($L_{Ref} = 2.5\ \mu$m and $D_{Ref} = 50$ nm) and longer high-L/D rods with $L/D = 400$ ($L_{Long} = 20\ \mu$m and $D_{Long} = D_{Ref}$) where the rod-length ratio is $r_L = L_{Long}/L_{Ref} = 8$. The proportion of longer rods in the network is expressed as a relative area fraction, $F_{Long} = AF_{Long}/(AF_{Ref} + AF_{Long})$, and is varied between $F_{Long} = 0$ (monodispesre; $L/D = 50$) and 1 (monodisperse; $L/D = 400$). As above, we use $R_{c\_effective} = 2\ k\Omega$ for all rod junctions in the network and the $R_{nw} = 0$.

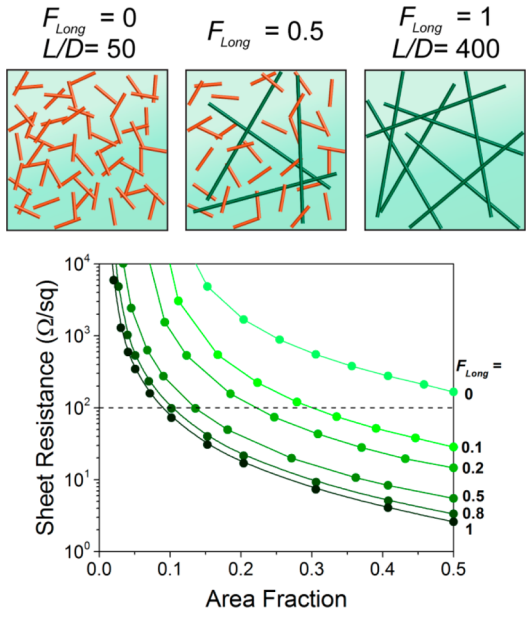

Figure 3. Simulated sheet resistance as a function of area fraction using $R_{c\_effective} = 2\ k\Omega$ for nanowire films composed of bidisperse mixtures of rods with $L/D = 50$ (Reference) and 400 (Long). The diameter is the same for both nanowire populations ($D_{Ref} = D_{Long} = 50$ nm), while the low- and high-aspect-ratio nanowires have lengths of 2.5 and 20 μm, respectively. Schematics illustrate networks with an increasing proportion of longer rods in the network as given by the relative area fraction of long rods, $F_{Long} = AF_{Long}/(AF_{Ref} + AF_{Long})$.

We plot the sheet resistance of these bidisperse rod networks as a function of the total area fraction for $F_{Long} = 0$, 0.2, 0.5, 0.8, and 1 (Figure 3). We observe a dramatic reduction in R_s by almost an order of magnitude when only 10% of rods have $L/D = 400$ nanowires. Subsequent increase in the fraction of high-L/D rods results in continued reduction of the film's R_s over 2 orders of magnitude. This promising result shows that bidisperse networks containing small fractions of high-L/D rods can be successful in forming films that meet desired performance criteria. Conversely, this data also shows that the presence of small amounts of low-L/D nanowires in a network of high-L/D nanowires ($F_{Long} = 0.8$) has a smaller impact on R_s. This finding is particularly encouraging as new synthetic methods for ultra-long nanowires have very high levels of size dispersity.[51,52] Beyond the bi-disperse example in Figure 3, our simulations can construct networks from rods with arbitrary distributions of rod length and diameter, including

experimental size distributions obtained from detailed characterization of nanowires. Also building on our work in 3D rod networks,[39] our simulations can readily incorporate nonisotropic orientation distributions that might result from shear or extensional flow during processing.

Constructing %*T versus* R_s Plot. Transparent conductors for high performance applications must display both a low sheet resistance ($R_s \leq 100$ Ω/sq) and high optical transparency (%$T > 90$%). Optimizing these two properties simultaneously is challenging as better transmittance requires reducing the area fraction of nanowires, while decreasing area fraction increases the sheet resistance. This highlights the great value of a computational framework for predicting how nanowire properties and network structure affect both of these parameters to guide future experimental work. Bergin *et al.*[15] recently studied the optical properties of silver nanowire films *via* experiments and FDTD simulations, reporting a linear relationship between network transmittance and area coverage of nanowires for a given D_{nw}. Moreover, the optical properties were determined to be independent of the nanowire length, in agreement with another recent study by Sorel *et al.*[31] Specifically, Bergin *et al.* found the following empirical relationship between the area fraction (AF) and the optical transmittance at $\lambda = 550$ nm:

$$\%T = 100 - a_1 \mathrm{AF} \quad (1)$$

where a_1 is a fitting parameter that accounts for the diameter and wavelength-dependent optical properties of the nanowires. For nanowires with $D_{nw} \approx 40$ nm, they found that $a_1 = 87$. By combining this empirical expression and simulated R_s values using $R_{c\_effective} = 2$ kΩ, Figure 4 predicts both the %T and R_s dependence on the nanowire length (at fixed $D_{nw} = 40$ nm) and area fraction.

Figure 4 is the first fully calculated plot of %T *vs* R_s in thin-film nanowire networks. Note that on a given curve (fixed L/D) each point represents a specific area fraction. While larger L/D is always advantageous for increasing %T at a fixed R_s, intermediate area fractions are needed to produce Ag NW films that achieve both %$T > 90$% and $R_s \leq 100$ Ω/sq. For example for $L/D = 800$, the high R_s results correspond to low areal density with high %T, while the lower R_s results correspond to higher areal density with low %T. At intermediate areal densities, both R_s and %T are in the high performance range of $R_s \leq 100$ Ω/sq and %$T > 90$%. For the Ag NWs of this study, Figure 4 shows that Ag NWs with high $L/D > 400$ are the most viable candidates for high performance transparent conductors. For $L/D > 400$, R_s and %T are both optimized over a very narrow range of intermediate area fractions AF ~ 0.05−0.1, demonstrating the strong sensitivity of the network performance on the nanowire area coverage. Thus, it is imperative that experimentalists characterize and report nanowire area fractions or areal densities, as well as nanowire dimensions and their distributions, alongside R_s and %T results to facilitate comparison between research groups and accelerate progress in the field.

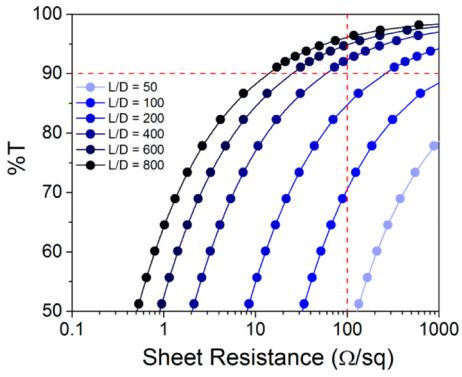

Figure 4. Calculated transmittance *vs* simulated sheet resistance for silver nanowire films for L/D ranging between 50 and 800 with $R_{c\_effective} = 2$ kΩ and constant $D_{nw} = 40$ nm. Optical transmittance values were calculated using the published empirical expression in eq 1. Dashed lines indicate desired performance criteria %$T > 90$% and $R_s \leq 100$ Ω/sq for high performance applications.

The results in Figure 4 are consistent with various experimental results in the literature. Bergin *et al.*[15] reported their best performance just shy of the desired $R_s \leq 100$ Ω/sq at 90% optical transmittance for networks of silver nanowires with $L/D = 375$. Similarly, Cambrios Technology Corp., whose proprietary ClearOhm transparent conductor material has recently been integrated into several commercially available touch screen devices, reports high performance films of silver nanowires with high $L/D \approx 550$ observing R_s as low as 30 Ω/sq at 90% transmittance.[27] Finally, Lee *et al.*[24] also report very high-performance silver nanowire films achieving $R_s < 20$ Ω/sq at 90% transmittance for very long silver nanowires with $L/D \approx 600$. For nanowire films with $D_{nw} < 100$ nm, the results in Figure 4 show the dual importance of area fraction and L/D in determining TC performance.

Comparison to the Percolative Figure of Merit. The optoelectrical properties of traditional transparent conductors are described by combining the physical expressions for transmittance and sheet resistance of bulk-like films[7,32]

$$T = \left[1 + \frac{Z_0}{2R_s}\frac{\sigma_{op}}{\sigma_{dc,B}}\right]^{-2} \quad (2)$$

where Z_0 is the impedance of free space (377 Ω), σ_{op} is the optical conductivity, and $\sigma_{dc,B}$ is the bulk dc conductivity of the film. The term $\sigma_{op}/\sigma_{dc,B}$ is known as the conductivity ratio and is often used as a figure of merit (FOM) to compare various material systems for TCs, whereby higher values of $\sigma_{op}/\sigma_{dc,B}$ correspond to better T *vs* R_s performance. Recently, Coleman and coworkers[3,32] observed a deviation from the expected bulk-like behavior eq 2 in nanowire and nanotube films

below a critical film thickness, t_{min}. They attribute this discrepancy to percolation effects in very thin films of nanoparticles, and modify eq 2 by incorporating terms that approximate the power-law dependence of the conductivity on thickness in the percolative regime,[32]

$$T = \left[1 + \frac{1}{\Pi}\left(\frac{Z_0}{R_s}\right)^{1/(n+1)}\right]^{-2} \quad (3a)$$

$$\Pi = 2\left[\frac{\sigma_{op}/\sigma_{dc,B}}{(Z_0 t_{min}\sigma_{op})^n}\right]^{1/(n+1)} \quad (3b)$$

where Π is their percolative FOM and $t_{min} \approx 2.33D$ is the film thickness below which the dc conductivity becomes thickness dependent (D is the diameter of the nanoparticle). The bulk-like and percolative FOMs are extracted by fitting experimental data to eqs 2 and 3, respectively. On a log−log plot of $T^{-1/2} - 1$ *vs* R_s, a slope of −1 is consistent with bulk-like behavior, while percolative behavior exhibits a less negative slope. On the basis of their percolative model in eq 3, they conclude that the main requirements for a good TC are high values of Π and low values of t_{min}, which in turn corresponds to minimizing the nanoparticle diameter since $t_{min} \approx 2.33D$. Further, the application of their percolative model to T *vs* R_s data for a wide range of metal- and carbon-based films reported in the literature showed that metal nanowire systems generally outperform carbon-based materials yielding higher Π values. While these findings are insightful, their semiempirical approach fails to account directly for nanoparticle dimensions (L and D) and network structure (area fraction), both of which strongly govern the performance in thin nanowire films as shown above. In addition, the single structural parameter cited in their model, namely, the effective film thickness, is ambiguous for nanowire films.[16,31]

To test the efficacy of their percolative model in capturing T *vs* R_s behavior in films of nanostructured materials, we fit eq 3 to our simulated R_s and calculated %T data (from Figure 4) for representative L/D across a large AF range in Figure 5. Figure 5 also includes experimental data for Ag NW films from Figure 1, which agrees very well with corresponding simulation and calculated data. The published empirical %T *vs* AF expression in eq 1 applies for Ag NWs with $D_{nw} = 40$ nm, so we fit experimental data to extract a new value of the fitting parameter $a_1 = 82$ corresponding to $D_{nw} = 75$ nm to use for the $L/D = 275$ data in Figure 5 (Figure SI-4). Table 1 summarizes the network structure parameters, as well as the percolative FOM (Π) and n values extracted from eq 3 fits to our data. Note that eq 3 could not be used to fit the entire range of AF, so two sets of fitting parameters are provided.

Several important observations arise from inspection of Figure 5 and Table 1. First, our simulations and experiments are inconsistent with predicted "bulk-like" behavior eq 2 for dense networks at high areal coverage.

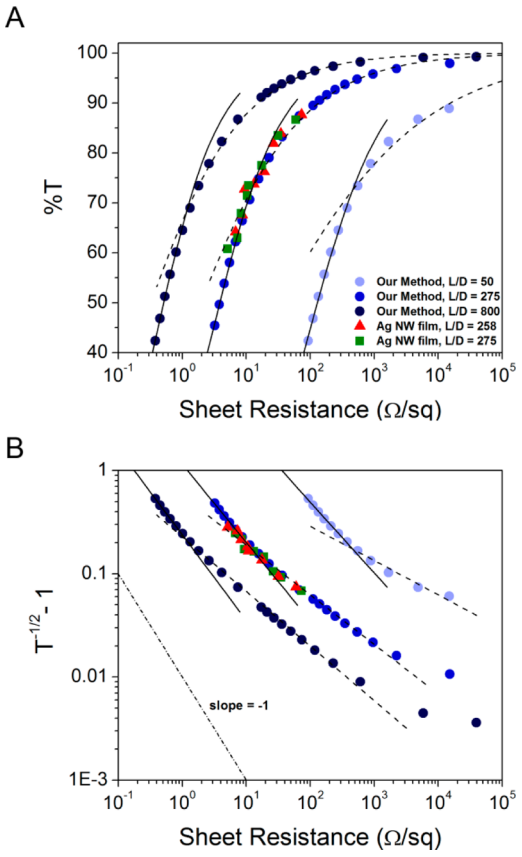

Figure 5. (A) Calculated transmittance *vs* simulated sheet resistance (circles) for silver nanowire films with L/D = 50 (D_{nw} = 40 nm), 275 (D_{nw} = 75 nm), and 800 (D_{nw} = 40 nm). $R_{c\_effective}$ = 2 kΩ for simulated sheet resistance data and optical transmittance values are calculated using eq 1 with a_1 = 87 and 82 for D_{nw} = 40 and 75 nm, respectively. Lines represent fits to the data using De *et al.*'s percolative model (eq 3) for networks with low to intermediate (AF < 0.4, dashed lines) and high (AF > 0.4, solid lines) nanowire areal density. Also shown are experimental results (triangles and squares) replotted from Figure 1 for Ag NW films with L/D = 258 (D_{nw} = 84 nm) and 275 (D_{nw} = 75 nm), respectively. (B) Data from (A) are replotted as $T^{-1/2} - 1$ *vs* R_s to fit eq 3 and find the percolative FOM (Π) and n. For comparison, the bulk-like behavior of eq 2 is represented by a slope of −1, while the data exhibit less negative slopes.

TABLE 1. Values of the Percolative FOM (Π) and n Obtained from eq 3 Fits to Calculated Transmittance *vs.* Simulated Sheet Resistance Data in Figure 5

			Our Method			De *et al.* Percolative Model[32]		
				$R_{c\_effective}$		AF range		perc. FOM
L/D	L (μm)	D (nm)		(kΩ)	AF	for fit	n	(Π)
50	2	40		2	0.13−0.66	0.13−0.36	2.01	5.39
						0.36−0.66	0.46	5.03
275	20.6	75		2	0.025−0.66	0.04−0.41	1.08	30.28
						0.41−0.66	0.32	78.27
800	32	40		2	0.008−0.66	0.02−0.46	0.89	101.19
						0.46−0.66	0.21	573.67

In Figure 5B, a slope of −1 is indicative of bulk-like behavior, while we observe slopes ranging between −0.3 and −0.8 in all cases. Thus, dense nanowire films do not behave like homogeneous films as percolation effects continue to dominate at areal densities as high as 70%. This is consistent with our finding in Figure 2 wherein L/D is critical in determining the R_s across the entire AF range, highlighting the importance of network structure even for dense networks. Additionally, eq 3 fails to capture our data over the entire AF range of interest. The percolative model fits the data only over narrow area fraction ranges such that multiple values for Π and n result for one type of nanowire film. Specifically, separate fits are required for nanowire networks with low to intermediate (AF < 0.4) and high (AF > 0.4) nanowire areal densities. In addition, very dilute networks with the highest transmittance and sheet resistance values (AF < 0.04 and 0.02 for L/D = 275 and 800, respectively) deviate from the dashed line fits in Figure 5, indicating that yet another set of percolative fitting parameters are required in this regime. Further, the resulting Π vary over an order of magnitude depending on L, D and AF for the same material system (Ag NW films), Table 1. Thus, this FOM is inadequate for evaluating and optimizing performance of TCs based on films of nanostructured materials.

The percolative FOM proposed by De *et al.* is an aggregate parameter that has the advantage of being simple to extract from experimental data, but is incomplete and misleading due to a failure to explicitly account for network morphology and topology. Our approach, which combines simulations of sheet resistance and calculation of the optical transmittance based on the empirical relationship between %T and AF, is more complete by encompassing the various attributes that can be independently controlled to optimize the TC performance. For isotropic nanowire films, we show that the main parameters that determine %T *vs* R_s behavior are L, D, AF, and the average effective contact resistance between the conductive fillers, see Figures 1, 2, and 4. Each of these four attributes can be controlled independently to optimize performance. Our approach is more complex as it requires an expression for the optical transmittance as a function of nanowire areal coverage, as well as simulations to extract $R_{c\_effective}$. For Ag NW films processed comparably to those presented in Figure 1 and with $L_{nw} < 20\,\mu$m and $D_{nw} \approx 40-100$ nm, Figures 2 and 4 give complete guidance on the optimal L/D and AF ranges that produce films with desired performance for specific applications. Our approach can be readily extended to evaluate and predict properties for new nanowire materials or new nanowire processing methods designed to reduce $R_{c\_effective}$. Further, our approach can explore the impact of changing L, D, and AF independently to optimize properties.

CONCLUSION

For metal nanowire thin films to compete as transparent conductors, predictive models of their optoelectronic properties are needed. This paper establishes a method that combines experimental sheet resistances, simulations that compute the sheet resistance, and empirical expressions for optical transparency to provide the first fully calculated plots of %T *versus* R_s. Our method can be broadly applied to nanoparticle systems to predict the impact of nanowire structure (length, diameter, size dispersity, *etc.*) and network morphology (areal density, dispersion, orientation, *etc.*) on network properties. Our many parameter approach promises to be more insightful and more rigorous than the widely used bulk-like and percolative figures of merit that combine the effects of L, D, AF, and $R_{c\_effective}$ in a way that makes it difficult understand or optimize performance.

The method was developed and demonstrated here for silver nanowire networks; we extract an average effective contact resistance of $R_{c\_effective}$ = 2 kΩ and clearly show that increasing the average L/D or adding a small fraction of high-L/D nanowires is paramount for reducing R_s at any area fraction. Specifically, silver nanowires of D_{nw} = 40 nm require $L/D > 400$ to optimize both the sheet resistance ($R_s \leq$ 100 Ω/sq) and optical transmittance (%T > 90%) for high performance applications. The clear advantages of increasing L/D should motivate new synthetic methods, while the sensitivity of R_s to areal density and dispersity in L requires rigorous characterization of nanowires and nanowire films to produce consistent properties.

Decreasing the contact resistance between nanowires or nanotubes is also a valuable approach for improving nanoparticle film performance. By providing a means to extract the average effective contact resistance from experimental results, our integrated approach enables the rigorous comparison of various strategies for decreasing contact resistance including removing organic dispersion agents, thermal treatments to increase contact area, and alloying nanowires to avoid surface oxides.[11,14,18,22,49] When the dimensions of the nanoparticles and the areal density of the films are known, our methodology can be applied to extract $R_{c\_effective}$ from R_s data. Moreover, the $R_{c\_effective}$ extracted from R_s measurements can be made directly on the as-processed films, rather than a specially fabricated crossed-nanowire sample.

Our simulations have quantified the interplay between the most critical parameters that govern performance in nanowire films, as well as set an important precedent in achieving quantitative correspondence between experiments and simulations in nanowire films. The next-generation simulations will incorporate the resistance of the nanowires, which is expected to

be increasingly important with higher aspect ratio nanowires. In addition, we can simulate nanowire systems with nonisotropic nanowire orientations to mimic anistropic morphologies that might result from a continuous, solvent-based fabrication method of nanowire films.

METHODS

Simulation Methods. A random configuration of straight, soft-core (*i.e.*, interpenetrable), cylindrical rods is generated in a supercell of dimensions 1 unit × 1 unit × h. Confinement is achieved by defining the height of the supercell $h = D_{rod}$, where D_{rod} is the diameter of the rods. The rods have isotropic orientation about z-axis but are confined in the $x-y$ plane. For each simulated network, the rods have constant D_{rod}, while the rod lengths vary depending on the specified aspect ratio (L/D). Simulations were performed for each condition at a range of rod densities defined by the volume fraction (ϕ). We compute the area fraction (AF) of our quasi-2D networks based on the projected area of a rod ($L_{rod} \times D_{rod}$), specifically AF = $4\phi/\pi$. This definition of AF is most consistent with our experiments. Simulations involve ~1000−420 000 rods depending on the prescribed ϕ and L/D. The supercell is divided into tiling sub-blocks, whose length is greater than the rod length, and rods that fall into each sub-block are registered. Aided by the sub-block data structures, the possible neighbors of each rod are determined with computational complexity that scales linearly with the total number of rods. Then, the shortest distance between the centers of two neighboring rods is calculated using a close-formed formula and when this distance is < D_{rod} the rods are in contact. A clustering analysis is then carried out to identify a percolating cluster of contacting rods that spans across the supercell, while non-percolating clusters are ignored. Every rod i in the percolating cluster is assigned a uniform voltage V_i (no internal resistance; $R_{rod} = 0$) that is an unknown variable, except for those rods that touch the left ($V_i = 1$) or right ($V_i = 0$) edges of the supercell. Assuming that all electrical resistance results from contact resistance, R_c, between contacting rods and writing Kirchoff's current law at each rod−rod junction, a system of linear equations is established. This system of linear equations is solved using the preconditioned conjugate gradient iterative (KSPCG) method[53] as implemented in the Portable, Extensible Toolkit for Scientific Computation (PETSc) package, where the incomplete LU factorization preconditioner (PCILU) is used, to obtain the cluster conductance. This entire procedure is repeated to obtain an ensemble-averaged conductance, achieving a standard deviation of less than 10% of the mean value in all cases. The resistivity of the rod ensemble is calculated by dividing the voltage drop (= 1 V) by the total current and normalizing by the dimensions of the supercell. For correspondence between simulation and physical units, we set $D_{rod} = D_{nw}$, where D_{nw} is the diameter of silver nanowires from experiments, and we divide the simulated resistivity by the film thickness (= D_{rod}) to obtain the sheet resistance.

Experimental Methods. Silver nanowires (Ag NWs) were synthesized using the polyol process as previously reported.[15,54] The nanowire solution was diluted with deionized water and purified through centrifugation multiple times to remove excess polyvinylpyrrolidone and other unwanted materials before being suspended and stored in water. Three batches of silver nanowires were synthesized having diameters of 50, 84, and 75 nm, corresponding to nanowires with L/D = 200, 258, and 275, respectively. Dimensions were measured by SEM. Known volumes of the suspension were filtered onto membranes and immediately transferred to polydimethylsiloxane films, producing nanowire films with varying nanowire area fractions. The sheet resistances of the Ag NW films were then measured using a four-point probe.

Conflict of Interest: The authors declare no competing financial interest.

Acknowledgment. This work was supported primarily by the MRSEC program of the National Science Foundation under award no. DMR-11- 20901, and by the University Research Foundation of the University of Pennsylvania. The authors acknowledge Prof. Ju Li of the Department of Nuclear Science and Engineering at M.I.T. for the generous use of his group's computer cluster. B.J.W. acknowledges financial support from NSF CAREER (DMR-1253534). A.R.R. was supported by a Paul M. Gross Fellowship from the Department of Chemistry at Duke University, and a fellowship from the NSF's Research Triangle MRSEC (DMR-1121107).

Supporting Information Available: Additional figures showing renderings of the rod networks from the quasi-2D simulations, percolation conductivity scaling fits to experimental sheet resistance data for silver nanowire films, simulated sheet resistance predictions over a larger areal density range, and empirical fit to transmittance *vs* areal coverage experimental data for Ag NWs with L/D = 275 and D_{nw} = 75 nm. This material is available free of charge *via* the Internet at http://pubs.acs.org.

REFERENCES AND NOTES

1. Hecht, D. S.; Hu, L. B.; Irvin, G. Emerging Transparent Electrodes Based on Thin Films of Carbon Nanotubes, Graphene, and Metallic Nanostructures. *Adv. Mater.* **2011**, *23*, 1482–1513.
2. Gordon, R. G. Criteria for Choosing Transparent Conductors. *MRS Bull.* **2000**, *25*, 52–57.
3. De, S.; Coleman, J. N. The Effects of Percolation in Nanostructured Transparent Conductors. *MRS Bull.* **2011**, *36*, 774–781.
4. U.S. Geological Survey. Mineral Commodity Summaries. Indium. *U.S. Geological Survey. Mineral Commodity Summaries. Indium.*; U.S. Department of the Interior: Washington, D.C., **2012**; p 74.
5. Kirchmeyer, S.; Reuter, K. Scientific Importance, Properties and Growing Applications of Poly(3,4-ethylenedioxythiophene). *J. Mater. Chem.* **2005**, *15*, 2077–2088.
6. Elschner, A.; Lovenich, W. Solution-Deposited Pedot for Transparent Conductive Applications. *MRS Bull.* **2011**, *36*, 794–798.
7. Hu, L.; Hecht, D. S.; Gruner, G. Percolation in Transparent and Conducting Carbon Nanotube Networks. *Nano Lett.* **2004**, *4*, 2513–2517.
8. Wu, Z. C.; Chen, Z. H.; Du, X.; Logan, J. M.; Sippel, J.; Nikolou, M.; Kamaras, K.; Reynolds, J. R.; Tanner, D. B.; Hebard, A. F.; *et al.* Transparent, Conductive Carbon Nanotube Films. *Science* **2004**, *305*, 1273–1276.
9. Zhou, Y. X.; Hu, L. B.; Gruner, G. A Method of Printing Carbon Nanotube Thin Films. *Appl. Phys. Lett.* **2006**, *88*, 123109.
10. Geng, H. Z.; Kim, K. K.; So, K. P.; Lee, Y. S.; Chang, Y.; Lee, Y. H. Effect of Acid Treatment on Carbon Nanotube-Based Flexible Transparent Conducting Films. *J. Am. Chem. Soc.* **2007**, *129*, 7758–7759.
11. Li, X.; Gittleson, F.; Carmo, M.; Sekol, R. C.; Taylor, A. D. Scalable Fabrication of Multifunctional Freestanding Carbon Nanotube/Polymer Composite Thin Films for Energy Conversion. *ACS Nano* **2012**, *6*, 1347–1356.
12. Wassei, J. K.; Kaner, R. B. Graphene, a Promising Transparent Conductor. *Mater. Today* **2010**, *13*, 52–59.
13. Bae, S.; Kim, H.; Lee, Y.; Xu, X.; Park, J.-S.; Zheng, Y.; Balakrishnan, J.; Lei, T.; Ri Kim, H.; Song, Y. I.; *et al.* Roll-to-Roll Production of 30-inch Graphene Films for Transparent Electrodes. *Nat. Nanotechnol.* **2010**, *5*, 574–578.
14. Lee, J. Y.; Connor, S. T.; Cui, Y.; Peumans, P. Solution-Processed Metal Nanowire Mesh Transparent Electrodes. *Nano Lett.* **2008**, *8*, 689–692.

15. Bergin, S. M.; Chen, Y. H.; Rathmell, A. R.; Charbonneau, P.; Li, Z. Y.; Wiley, B. J. The Effect of Nanowire Length and Diameter on the Properties of Transparent, Conducting Nanowire Films. *Nanoscale* **2012**, *4*, 1996–2004.
16. De, S.; Higgins, T. M.; Lyons, P. E.; Doherty, E. M.; Nirmalraj, P. N.; Blau, W. J.; Boland, J. J.; Coleman, J. N. Silver Nanowire Networks as Flexible, Transparent, Conducting Films: Extremely High DC to Optical Conductivity Ratios. *ACS Nano* **2009**, *3*, 1767–1774.
17. Leem, D. S.; Edwards, A.; Faist, M.; Nelson, J.; Bradley, D. D. C.; de Mello, J. C. Efficient Organic Solar Cells with Solution-Processed Silver Nanowire Electrodes. *Adv. Mater.* **2011**, *23*, 4371–4375.
18. Hu, L. B.; Kim, H. S.; Lee, J. Y.; Peumans, P.; Cui, Y. Scalable Coating and Properties of Transparent, Flexible, Silver Nanowire Electrodes. *ACS Nano* **2010**, *4*, 2955–2963.
19. Madaria, A. R.; Kumar, A.; Zhou, C. W. Large Scale, Highly Conductive and Patterned Transparent Films of Silver Nanowires on Arbitrary Substrates and Their Application in Touch Screens. *Nanotechnology* **2011**, *22*, No. 245201.
20. Zeng, X. Y.; Zhang, Q. K.; Yu, R. M.; Lu, C. Z.; New Transparent, A. Conductor: Silver Nanowire Film Buried at the Surface of a Transparent Polymer. *Adv. Mater.* **2010**, *22*, 4484–4488.
21. Rathmell, A. R.; Wiley, B. J. The Synthesis and Coating of Long, Thin Copper Nanowires to Make Flexible, Transparent Conducting Films on Plastic Substrates. *Adv. Mater.* **2011**, *23*, 4798–4803.
22. Rathmell, A. R.; Nguyen, M.; Chi, M.; Wiley, B. J. Synthesis of Oxidation-Resistant Cupronickel Nanowires for Transparent Conducting Nanowire Networks. *Nano Lett.* **2012**, *12*, 3193–3199.
23. Wu, H.; Hu, L. B.; Rowell, M. W.; Kong, D. S.; Cha, J. J.; McDonough, J. R.; Zhu, J.; Yang, Y. A.; McGehee, M. D.; Cui, Y. Electrospun Metal Nanofiber Webs as High-Performance Transparent Electrode. *Nano Lett.* **2010**, *10*, 4242–4248.
24. Lee, J.; Lee, P.; Lee, H.; Lee, D.; Lee, S. S.; Ko, S. H. Very Long Ag Nanowire Synthesis and Its Application in a Highly Transparent, Conductive and Flexible Metal Electrode Touch Panel. *Nanoscale* **2012**, *4*, 6408–6414.
25. Kumar, A.; Zhou, C. The Race to Replace Tin-Doped Indium Oxide: Which Material Will Win? *ACS Nano* **2010**, *4*, 11–14.
26. Canbrios Home Page. http://www.cambrios.com/Technology/.
27. Sepa, J.; Wallace, F. Low-Haze Transparent Conductors. U.S. Patent 2011/0174190 A1, July 21, 2011.
28. Li, J.; Zhang, S.-L. Conductivity Exponents in Stick Percolation. *Phys. Rev. E* **2010**, *81*, 021120.
29. Li, J. T.; Zhang, S. L. Finite-Size Scaling in Stick Percolation. *Phys. Rev. E* **2009**, *80*, 040104.
30. Pike, G. E.; Seager, C. H. Percolation and Conductivity: A Computer Study. I. *Phys. Rev. B* **1974**, *10*, 1421–1434.
31. Sorel, S.; Lyons, P. E.; De, S.; Dickerson, J. C.; Coleman, J. N. The Dependence of the Optoelectrical Properties of Silver Nanowire Networks on Nanowire Length and Diameter. *Nanotechnology* **2012**, *23*, 185201.
32. De, S.; King, P. J.; Lyons, P. E.; Khan, U.; Coleman, J. N. Size Effects and the Problem with Percolation in Nanostructured Transparent Conductors. *ACS Nano* **2010**, *4*, 7064–7072.
33. Behnam, A.; Guo, J.; Ural, A. Effects of Nanotube Alignment and Measurement Direction on Percolation Resistivity in Single-Walled Carbon Nanotube Films. *J. Appl. Phys.* **2007**, *102*, 044313.
34. Kocabas, C.; Pimparkar, N.; Yesilyurt, O.; Kang, S. J.; Alam, M. A.; Rogers, J. A. Experimental and Theoretical Studies of Transport through Large Scale, Partially Aligned Arrays of Single-Walled Carbon Nanotubes in Thin Film Type Transistors. *Nano Lett.* **2007**, *7*, 1195–1202.
35. Kumar, S.; Murthy, J. Y.; Alam, M. A. Percolating Conduction in Finite Nanotube Networks. *Phys. Rev. Lett.* **2005**, *95*, 066802.
36. Žeželj, M.; Stanković, I. From Percolating to Dense Random Stick Networks: Conductivity Model Investigation. *Phys. Rev. B* **2012**, *86*, 134202.
37. Keblinski, P.; Cleri, F. Contact Resistance in Percolating Networks. *Phys. Rev. B* **2004**, *69*, 184201.
38. Kirkpatrick, S. Percolation and Conduction. *Rev. Mod. Phys.* **1973**, *45*, 574–588.
39. White, S. I.; DiDonna, B. A.; Mu, M. F.; Lubensky, T. C.; Winey, K. I. Simulations and Electrical Conductivity of Percolated Networks of Finite Rods with Various Degrees of Axial Alignment. *Phys. Rev. B* **2009**, *79*, 024301.
40. White, S. I.; Mutiso, R. M.; Vora, P. M.; Jahnke, D.; Hsu, S.; Kikkawa, J. M.; Li, J.; Fischer, J. E.; Winey, K. I. Electrical Percolation Behavior in Silver Nanowire-Polystyrene Composites: Simulation and Experiment. *Adv. Funct. Mater.* **2010**, *20*, 2709–2716.
41. Mutiso, R. M.; Sherrott, M. C.; Li, J.; Winey, K. I. Simulations and Generalized Model of the Effect of Filler Size Dispersity on Electrical Percolation in Rod Networks. *Phys. Rev. B* **2012**, *86*, 214306.
42. Balberg, I.; Anderson, C. H.; Alexander, S.; Wagner, N. Excluded Volume and Its Relation to the Onset of Percolation. *Phys. Rev. B* **1984**, *30*, 3933–3943.
43. Bug, A. L. R.; Safran, S. A.; Webman, I. Continuum Percolation of Rods. *Phys. Rev. Lett.* **1985**, *54*, 1412–1415.
44. Foygel, M.; Morris, R.; Anez, D.; French, S.; Sobolev, V. Theoretical and Computational Studies of Carbon Nanotube Composites and Suspensions: Electrical and Thermal Conductivity. *Phys. Rev. B* **2005**, *71*, 104201.
45. Neda, Z.; Florian, R.; Brechet, Y. Reconsideration of Continuum Percolation of Isotropically Oriented Sticks in Three Dimensions. *Phys. Rev. E* **1999**, *59*, 3717–3719.
46. White, S. I.; DiDonna, B. A.; Mu, M.; Lubensky, T. C.; Winey, K. I. Simulations and Electrical Conductivity of Percolated Networks of Finite Rods with Various Degrees of Axial Alignment. *Phys. Rev. B* **2009**, *79*, 024301.
47. Fuhrer, M. S.; Nygard, J.; Shih, L.; Foreror, M.; Yoon, Y.-G.; Mazzoni, M. S. C.; Choi, H. J.; Ihm, J.; Louie, S. G.; Zettl, A.; *et al.* Crossed Nanotube Junctions. *Science* **2000**, *288*, 494–497.
48. Mutiso, R. M.; Winey, K. I. Electrical Percolation in Quasi-2d Metal Nanowire Networks for Transparent Conductors. *Phys. Rev. E* **2013**, submitted for publication.
49. Garnett, E. C.; Cai, W.; Cha, J. J.; Mahmood, F.; Connor, S. T.; Christoforo, M. G.; Cui, Y.; McGehee, M. D.; Brongersma, M. L. Self-Limited Plasmonic Welding of Silver Nanowire Junctions. *Nat. Mater.* **2012**, *11*, 241–249.
50. Pike, G. E.; Seager, C. H. Percolation and Conductivity: A Computer Study. I*. *Phys. Rev. B* **1974**, *10*, 1421–1434.
51. Lee, P.; Lee, J.; Lee, H.; Yeo, J.; Hong, S.; Nam, K. H.; Lee, D.; Lee, S. S.; Ko, S. H. Highly Stretchable and Highly Conductive Metal Electrode by Very Long Metal Nanowire Percolation Network. *Adv. Mater.* **2012**, *24*, 3326–3332.
52. Zhang, D.; Wang, R.; Wen, M.; Weng, D.; Cui, X.; Sun, J.; Li, H.; Lu, Y. Synthesis of Ultralong Copper Nanowires for High-Performance Transparent Electrodes. *J. Am. Chem. Soc.* **2012**, *134*, 14283–14286.
53. Hestenes, M. R.; Stiefel, E. Methods of Conjugate Gradients for Solving Linear Systems. *J. Res. Natl. Bur. Stand.* **1952**, *49*, 410–436.
54. Wiley, B.; Sun, Y. G.; Xia, Y. N. Polyol Synthesis of Silver Nanostructures: Control of Product Morphology with Fe(Ii) or Fe(III) Species. *Langmuir* **2005**, *21*, 8077–8080.